THE UNIVERSITY *of* EDINBURGH

Edinburgh Research Explorer

Characterisation of a ruthenium bipyridyl dye showing a long-lived charge-separated state on TiO2 in the presence of I-/I3-

OPEN ACCESS

Characterisation of a Ruthenium Bipyridyl Dye Showing a Long-lived Charge-separated State on TiO$_2$ in the Presence of I$^-$/I$_3^-$**

Keri L. McCall,[1] Ana Morandeira,[2] James Durrant,[2] Lesley J. Yellowlees[1] and Neil Robertson[1,*]

[1]EaStCHEM, School of Chemistry, Joseph Black Building, University of Edinburgh, West Mains Road, Edinburgh, EH9 3JJ, UK.

[2]Department of Chemistry, Imperial College, London, UK.

[*]Corresponding author; e-mail: neil.robertson@ed.ac.uk; fax: +44 1316504743; tel: +44 1316504755

Supporting information:
[†]Electronic Supplementary Information (ESI) available: Fig. S1 CV studies of (SC$_2$H$_4$CN)$_2$TTF(SMe)$_2$; Fig. S2 Differential pulse study of **1**; Fig. S3 Differential pulse study of **2**; Fig. S4 Absorption spectrum of (SC$_2$H$_4$CN)$_2$TTF(SMe)$_2$; Fig. S5 Excitation and emission spectra of **1** and **2** at RT; Fig. S6 Excitation and emission spectra of **1** and **2** at 77 K; Fig. S7 Oxidative OTTLE study of (SC$_2$H$_4$CN)$_2$TTF(SMe)$_2$; Fig. S8 Oxidative OTTLE studies of **2**; Fig. S9 Reductive OTTLE studies of **2**; Table S1 Absorption spectra maxima of oxidised and reduced species; Fig. S10 Optimised geometry of **2**; Table S2 Calculated energies and percentage contributions of Ru, decbpy, TTF for selected orbitals of **2**; Fig. S11 I-V characteristics for DSSCs sensitised with **3**; Fig. S12 Absorption spectra of TiO$_2$ films sensitised with **3**. See http://dx.doi.org/10.1039/B924660F

Graphical abstract:
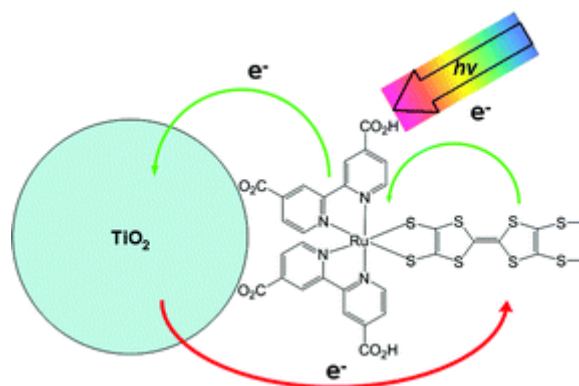
Abstract

The control of the loss mechanism in a dye sensitised solar cell (DSSC) via recombination of the injected electron with the oxidised dye was investigated by incorporating a redox-active ligand, 6,7-bis(methylthio)tetrathiafulvalene dithiolate ($TTF(SMe)_2$), into a ruthenium bipyridyl dye. A series of dyes with general formula [Ru(4,4′-R-bpy)$_2$($TTF(SMe)_2$], where R=H, CO_2Et and CO_2H, were synthesised and characterised using electrochemistry, absorption and emission spectroscopy, spectroelectrochemistry and hybrid-DFT calculations. In addition, the performance of the acid derivative in a DSSC was investigated using IV measurements, as well as transient absorption spectroscopy. These complexes showed significant TTF-ligand character to the HOMO orbital, as deduced by spectroelectrochemical, emission and computational studies. Upon adsorption of the acid derivative to TiO_2 a long-lived charge-separated state of 20 ms was observed via transient absorption spectroscopy. Despite this long-lived charge-separated state, the dye yielded extremely low DSSC efficiencies, attributed to the poor regeneration of the neutral dye by iodide. As a result, the complex forms a novel long-lived charge separated state that persists even under working solar cell electrolyte conditions.

Introduction

Dyes-sensitised solar cells (DSSC) have emerged as one of the most promising technologies for low-cost photovoltaics.[1] The study of electron transfer processes within a DSSC is crucial to optimising the efficiency of the system, as with this knowledge the various steps that occur within the cell can be further understood and eventually controlled. This should allow maximisation of the forward processes and reduction of the loss mechanisms. This paper discusses the molecular design of ruthenium polypyridyl complexes in order to study the interfacial charge recombination dynamics at the dye/TiO_2 heterojunction.

The strategy used in this study is that of a donor-acceptor dye (Fig. 1). In this system an electron donor moiety is covalently linked to a chromophore unit. Upon excitation of the chromophore by incident light, an electron is injected into the conduction band of the TiO_2 (1). This is rapidly followed by the transfer of an electron from the appended electron donor unit (2). This shifts the dye cation hole further from the surface of the TiO_2, leading to the recombination loss process (3) being significantly retarded.

There are several examples of mononuclear ruthenium polypyridyl dyes with appended secondary electron-donor units that show extended charge-separated state lifetimes in a DSSC. All of these examples utilise the wealth of bipyridyl chemistry by attaching the donor unit to the second or a third bipyridyl ligand. The use of known electron donors such as phenothiazines (PTZ) has resulted in charge-separated lifetimes of up to 300 μs, with the dye anchored on TiO_2. [2,3] Whereas the use of 4-[4-(*N,N*-di-*p*-anisylamino)phenoxymethyl]-4'-methyl-2,2'bipyridine in place of the second dcbpy ligand to yield a analogue (called N845) of the well-

known N3 dye ([Ru(dcbpy)$_2$(NCS)$_2$], dcbpy = 4,4´-CO$_2$H-2,2´-bipyridyl) showed a charge-separated lifetime of 0.7 s.[4] The latter study also investigated the nature of the MOs *via* semiempirical calculations, showing the HOMO to be located on the donor-substituted bipyridyl ligand hence the extended lifetime. Neither of these studies has reported global efficiency values for a DSSC.
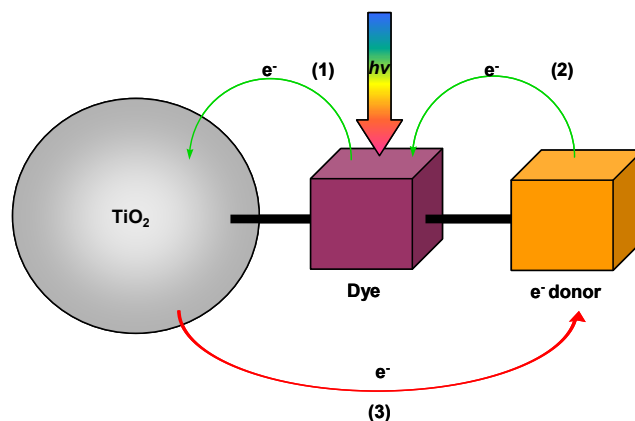
Figure 1. Schematic showing electron transfer processes occurring upon excitation of a donor-acceptor dye sensitised on TiO$_2$.

A series of dyes which has received significant attention recently is a ruthenium tris-bipyridyl triphenylamine (TPA) series.[5,6,7] By systematic variation of the third functionalised bipyridyl ligand the influence of extended π-conjugation, and also the use of polymeric electron-donating units on the charge-separated state in a DSSC were investigated. N3 analogues have also been investigated, where the functionalised bipyridyl ligand replaces one of the dcbpy ligands and the NCS groups are retained.[8,9,10] It was found that a dye with appended polymeric TPA groups had an extremely long-lived charge-separated state of 4 s when adsorbed to

TiO$_2$, measured *via* transient absorption spectroscopy. This is the longest charge-separated lifetime reported to date for a dye/TiO$_2$ system and was attributed, *via* DFT calculations, to the HOMO being entirely located over the triphenylamine units rather than on the ruthenium core. In addition these dyes have been found to perform significantly well in solid-state DSSCs, using spiro-OMeTAD as the electrolyte, with a maximum efficiency to date of 3.4 %.

The study above relates well to the conclusions of a previous report where the recombination dynamics of a number of ruthenium bipyridyl, phthalocyanine and porphyrin dyes were studied. This concluded that the recombination in these systems was strongly linked to the spatial separation of the dye cation HOMO from the

TiO$_2$ surface. Further to this it was calculated that a change in the spatial separation between these two components of just 3 Å results in a 10-fold change in the recombination half-time (t$_{1/2}$).[11]
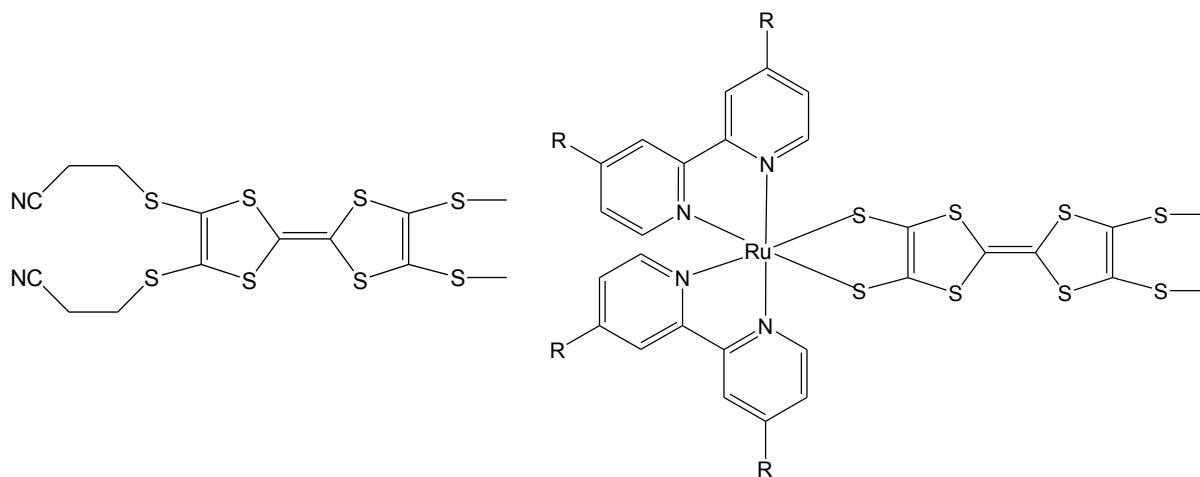

Figure 2. Structure of **(SC$_2$H$_4$CN)$_2$TTF(SMe)$_2$** (left) and dye series with general formula [Ru(4,4′-R-bpy)$_2$(TTF(SMe)$_2$] (right), where R = H (**1**), CO$_2$Et (**2**), CO$_2$H (**3**).

With these studies in mind, this work complexes a functionalised tetrathiafulvalene (TTF) unit to a ruthenium bipyridyl moiety (Fig. 2). Derivatised TTFs have long been of interest as functional molecules due to their unique electron donor properties. They are frequently used as building blocks for charge-transfer salts, yielding organic conductors and superconductors.[12] There are a wide variety of other applications that utilise TTF derivatives, including organic electronics,[13,14] magnetic materials[15] and supramolecular chemistry.[16,17]

With such a large range of applications there are numerous examples where a transition metal is complexed by a functionalised-TTF ligand, mainly of Cu,[18,19] Ni,[20,21] and Pt.[22,23,24] There are also examples of TTF-functionalised bipyridyl ligands18[,25,26] and a fused dipyridophenazine-TTF ligand with which ruthenium complexes have subsequently been synthesised.[27,28] The existing ruthenium complexes with appended TTF moieties all show some degree of electronic communication between the TTF and the ruthenium centre often leading to luminescence quenching. Only two examples exist where a TTF unit is directly bound,[29] or complexed[30] to the ruthenium. In one case a bis-TTF ruthenium trichloride complex was investigated, however in the other the TTF was bound to a Ru(bpy)$_2$ moiety via sulfur-donor atoms and primarily investigated for the electrical conductivity of the oxidised species.

This study aims to utilise the electron donating ability of the TTF unit to increase the lifetime of the charge-separated state of the dye in a DSSC, thereby reducing the recombination of the injected electron with the oxidised dye.

Results and Discussion

Synthesis

In general, the complexes were synthesised by treatment of the appropriate precursor [Ru(4,4´-R-bpy)$_2$Cl$_2$] with AgNO$_3$ to remove the Cl$^-$ ligands. The solution was then treated with [S$_2$TTF(SMe)$_2$]$^{2-}$ formed by *in situ* deprotection of the ligand precursor (SC$_2$H$_4$CN)$_2$TTF(SMe)$_2$ (**Pro-L**) by treatment with base.

Electrochemistry

Complexes **1** - **3** all show remarkably similar oxidation potentials (Table 1 and Fig. S2 - S3). This may reflect the similarity in nature of the occupied orbitals, *i.e.* the large contribution of **TTF(SMe)$_2$**. This point is further discussed with respect to the spectroelectrochemical and computational work. It should be noted that cyclic voltammetry studies of these complexes showed very poorly defined voltammograms, due to the three oxidations occurring at very similar potentials. Therefore in all cases differential pulse voltammetry was used to establish a more accurate description of the redox processes for these systems. See ESI for further information.

The reduction potentials of the complexes vary according to expectations, with **1** showing the more negative reductions relative to the complexes containing the electron withdrawing ester and acid derivatives (**2** and **3**). It should be noted that the electrochemical studies were also carried out in 0.3 M TBABF$_4$/DCM, however the oxidation potentials did not vary from those observed in DMF.

Table 1. Summary of redox potentials for **1**, **2**, **3** and (SC$_2$H$_4$CN)$_2$TTF(SMe)$_2$ (**Pro-L**) in 0.1 M TBABF$_4$/DMF (*vs.* Ag/AgCl).

Compound	$E_{1/2}^{ox}$ / V			$E_{1/2}^{red}$ / V	
Pro-L		0.85	0.71		
1 [a]	0.79	0.56	0.42	-1.41	-1.49
2 [a]	0.79	0.65	0.47	-1.01	-1.3
3 [a]	0.78	0.64	0.46	-0.98	

[a] Obtained *via* differential pulse experiment

Absorption Spectroscopy

The absorption spectra of complexes **1** – **3** (Fig. 3, Table 2) are somewhat unusual for ruthenium bipyridyl complexes in that they have very poorly defined bands in the visible region, with a gradual increase in

absorption from ~ 800 nm onwards. This broad absorption range would be advantageous, however the molar extinction co-efficients of the lower energy bands are relatively small (less than 9000 M^{-1} cm^{-1}). This means that the light harvesting ability of this dye is comparatively poor. The absorption spectrum is rather broad for this series of complexes due to the contribution the TTF moiety makes to the highest occupied orbitals, a point which is further discussed with respect to the computational work. It should also be noted that a broad absorption spectrum was observed for both previously studied complexes where TTF was covalently bound to a ruthenium centre.[29,30]
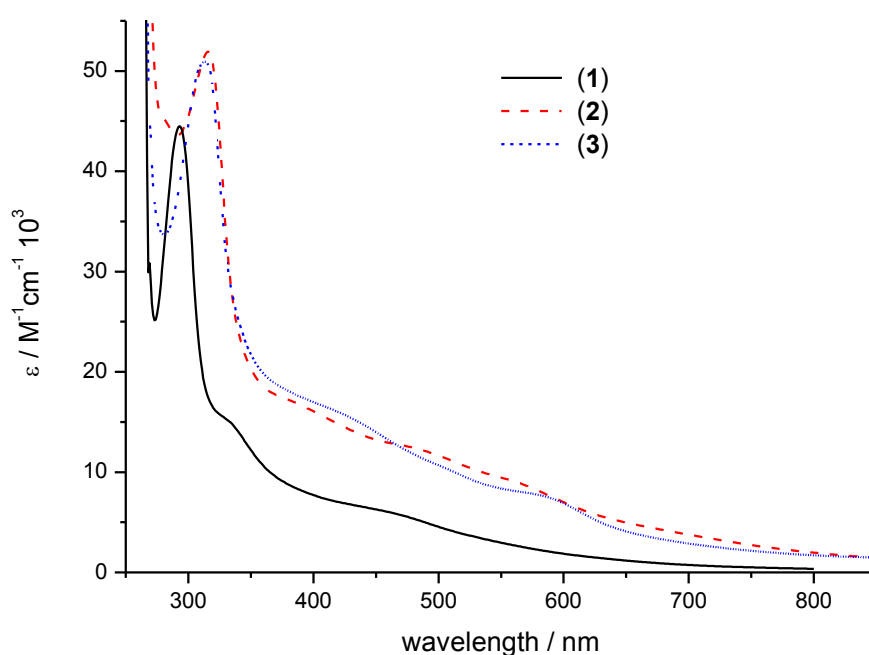
Figure 3. Absorption spectra of complexes **1 – 3** in DMF.

Emission Studies

The room temperature emission studies of **$(SC_2H_4CN)_2TTF(SMe)_2$** and complexes **1 – 3** are summarised in Fig. S5 and Table 3. **$(SC_2H_4CN)_2TTF(SMe)_2$** was found to yield no emission, in agreement with previous luminescence studies of functionalised TTF systems.[31] The observed emission in the studies of complexes **1 – 3** was found to be that of the chromophoric unit $Ru(R-bpy)_2$, as shown by the similarity of the emission maxima to those of $[Ru(R-bpy)_3]^{2+}$ for all three complexes.[32,33,34] This result suggests that the model of electron transfer processes outlined in Figure 1 may be an accurate representation for these complexes, as the two distinct units appear to retain to some extent their individual properties. It would be expected that the

lifetime of these emissions would be substantially reduced relative to the tris-(R-bpy) complexes (100s of nanoseconds) as the TTF moiety should facilitate rapid electron transfer to the Ru(R-bpy)$_2$ moiety and result in quenching of the emission. These observations have been made previously for a ruthenium complex incorporating a TTF functionalised bipyridyl ligand.[18] The fact that emission is observed at all suggests that the timescale of the intramolecular electron transfer is longer than or comparable with the intersystem crossing from the ^{1}MLCT state to the ^{3}MLCT state (which generally occurs on a sub-picosecond timescale)[35].

The excitation spectra for these complexes show the transitions which result in the emission. In this case they would be allowed transitions to ^{1}MLCT which relax (*via* intersystem crossing) to the emissive ^{3}MLCT states. The lack of overlap between the excitation and emission spectra is evidence for emission from the triplet state. The absence of broad absorption bands in the excitation spectra, as observed via absorption spectroscopy, indicates that there are transitions which relax non-radiatively for these complexes. These may involve transitions within the TTF moiety or orbitals which are largely mixed *i.e.* both Ru and TTF in character.

Emission studies of complexes **1** - **3** were also carried out at 77 K in frozen glass ethanol solutions. These exhibit very similar but more intense emission and excitation spectra, however there is greater resolution at lower temperature, especially for **2** which shows two sharp peaks at 77 K in place of a broad band at room temperature (Fig. S6).

Spectroelectrochemistry

OTTLE

The redox processes of **1** and **2** (Table S1) were followed spectroscopically using an optically-transparent thin layer electrode (OTTLE). Remarkably, this enabled the spectroscopic characterisation of six different redox states (overall charge of -2, -1, 0, +1, +2, +3) of the same complex, each of which was chemically stable under the cell conditions. The growth of a broad band between 9000 and 13000 cm^{-1} was observed after mono and di-oxidation of **1**. The intra-bipy band at 34000 cm^{-1} also decreases in intensity after both oxidations. The main difference between the two is the behaviour of the visible region bands at 22000 and 30000 cm^{-1}. The mono-oxidised species shows a partial collapse of the highest energy visible band but no change in the low energy band. However, the di-oxidised species shows a complete collapse of the high energy band accompanied by a growth of the low energy band. The origins of the changes in absorption with oxidation are further discussed in conjunction with the oxidative OTTLE studies of **2**, below. It should be noted that the tri-oxidised species of **1** was also studied but was found to be unstable in both DMF and DCM.

The oxidations of **2** were studied in both DMF and DCM, to investigate the reversibility of the various processes (Fig. S8). In both solvents the first and second oxidations were found to be fully reversible, however the third was only partially reversible in DMF and fully reversible in DCM.

The first two oxidations have similar effects on the absorption spectrum of **2**, showing the growth of a band at 9200 cm^{-1}, a decrease in intensity of the bipyridyl intraligand band at 32000 cm^{-1} and the increase of the MLCT band at 23000 cm^{-1}. The main difference between the two spectra is the appearance of a second low energy band at 13000 cm^{-1} for the di-oxidised species. The low energy bands may either be assigned to intraligand TTF transitions, as observed for **(SC$_2$H$_4$CN)$_2$TTF(SMe)$_2$** (Fig. S7), or to HOMO to LUMO transitions, as discussed further with respect to the computational work.

The tri-oxidised absorption spectrum shows a further growth in intensity of the low energy peaks at 14000 and 9200 cm^{-1}, however this is accompanied by the decrease in the MLCT band at 23000 cm^{-1} and a slight broadening of the intraligand band. These are typical responses for a ruthenium oxidation,[36] albeit not as pronounced as for most other ruthenium bipyridyl complexes, and so this third oxidation was tentatively assigned as based predominantly on the ruthenium centre. The fact that the first two oxidations showed very similar responses and that they resulted in the growth rather than collapse of the band assigned as an MLCT suggests that these oxidations are not based on the ruthenium centre, and were tentatively assigned as TTF based oxidations.

The reductive OTTLE studies of **2** showed typical mono-reduced and di-reduced species for a ruthenium bipyridyl complex (Fig S9), with the partial collapse of the bipyridyl intraligand band at 31000 cm^{-1} and the growth of three new bands at 6500, 19000 and 27000 cm^{-1} on mono-reduction. The bipyridyl intraligand band further collapses upon di-reduction and continued growth of the three new π-π* bands was observed. These studies indicate that the LUMO is located on the bipyridyl ligands as expected.

In-situ EPR

The mono-oxidation of **(SC$_2$H$_4$CN)$_2$TTF(SMe)$_2$** resulted in the growth of a single peak with g = 2.0197. Inducing the second oxidation resulted in the collapse of this new peak. This is entirely as expected for a functionalised TTF, with the single uncoupled peak showing that the unpaired electron is located on one of the central rings surrounded by elements with a nuclear spin of zero, rather than the peripheral methyl thiol or cyanoethylthio groups where there are non-zero nuclear spin elements.

The EPR studies of **2** showed the growth of a single uncoupled peak upon inducing the first oxidation with g = 2.0191. With di-oxidation the peak collapses to yield an EPR silent species and there is no return of a signal upon tri-oxidation. This provides further evidence for the first oxidation being TTF based, as the generation of an uncoupled signal with a g-factor very similar to that of oxidised **(SC$_2$H$_4$CN)$_2$TTF(SMe)$_2$** can only account for an unpaired electron being located on the TTF ligand. The studies do not discern between the nature of the second and third oxidations, however as the collapse of the peak could result from either the ruthenium or the second TTF based oxidation.

The lack of any observable signal with the oxidation of the ruthenium (whether it be the second or third) is not wholly unexpected. Ruthenium has two non-zero spin isotopes ^{99}Ru and ^{101}Ru, both with I = 5/2. It may be expected that upon oxidation of the ruthenium centre the resulting d^5 Ru(III) would be EPR active. This is often not the case, however, as spin-orbit coupling leads to rapid relaxation due to the strong orbital contribution to the magnetic moment.

Overall these spectroelectrochemical studies have shown that this system has the potential to show long-lived charge-separated lifetimes in a DSSC as the HOMO appears to be located largely on the TTF ligand.

Hybrid DFT Calculations

Computational calculations involving **2** also proved to be very informative about the nature of the numerous oxidations occurring with this complex. The calculated occupied orbitals (Fig. 4, Table S2) relate very well to the experimentally observed phenomena. The HOMO and HOMO-1 show only a small contribution from the ruthenium centre with the majority of the orbital found to be localised on the TTF ligand. The HOMO-2 showed a much larger ruthenium contribution to the orbital with a smaller degree of TTF nature. These results agree very well with the spectroelectrochemical studies and once again suggest that the first oxidation is TTF in nature, which indicates that this system may show significantly increased charge-separation in a DSSC. The LUMO and further unoccupied orbitals were calculated to be largely based on the two bipyridyl ligands with a small contribution from the ruthenium, which also relates very well to the reductive OTTLE study conclusions.

(a)

(b)

(c)

(d)
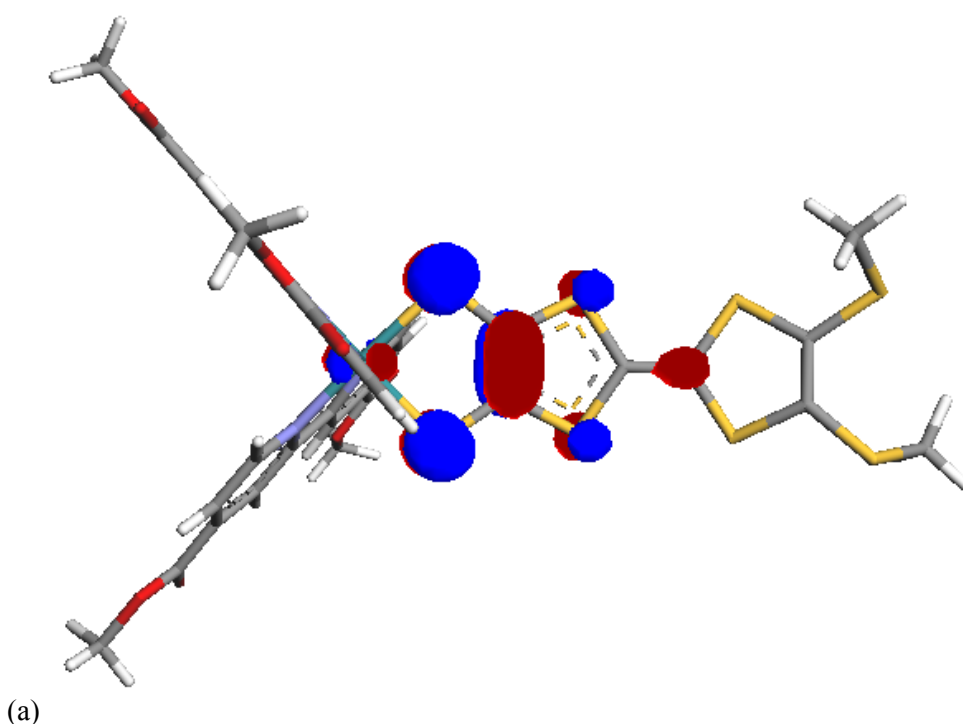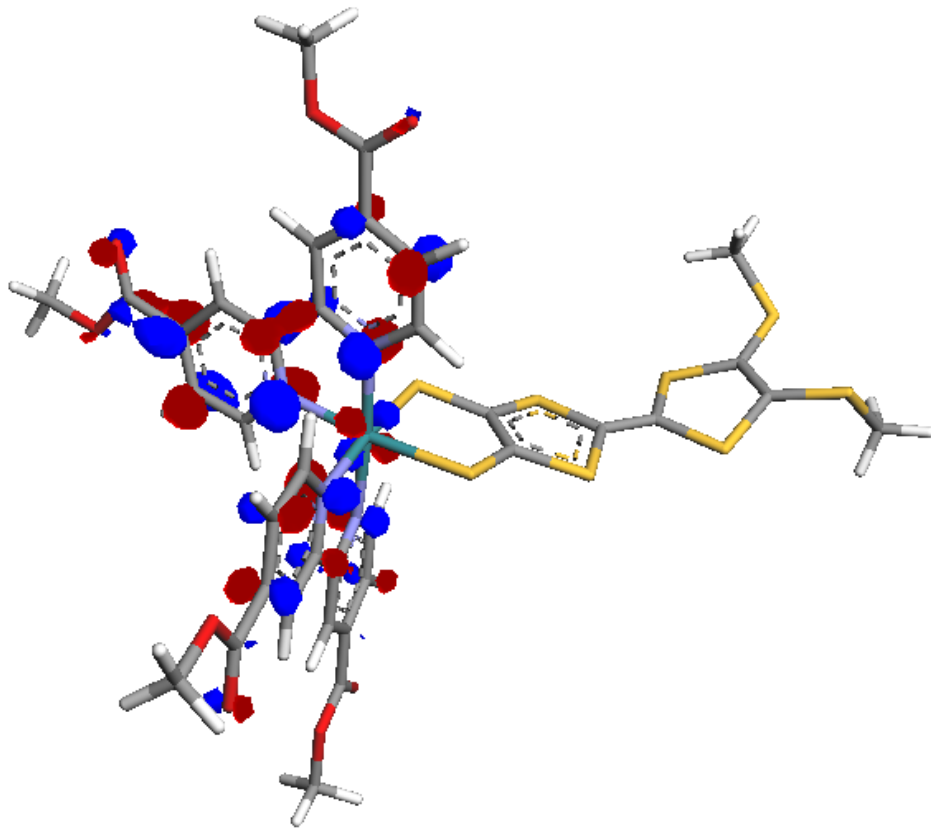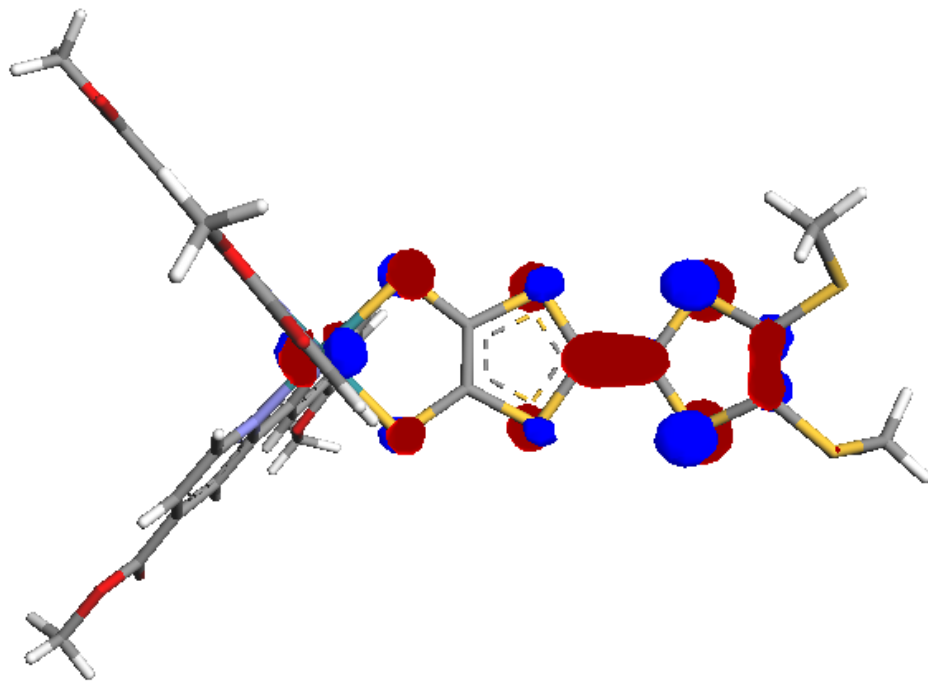
Figure 4. Hybrid DFT calculated HOMO (a), HOMO-1 (b), HOMO-2 (c) and LUMO (d) of **2** using a DMF polarisable continuum model.

Time-dependent DFT Calculations

To simulate the full absorption spectrum of **2**, 70 singlet-singlet transitions were calculated using the optimised geometry in a DMF polarisable continuum model (Fig 5). 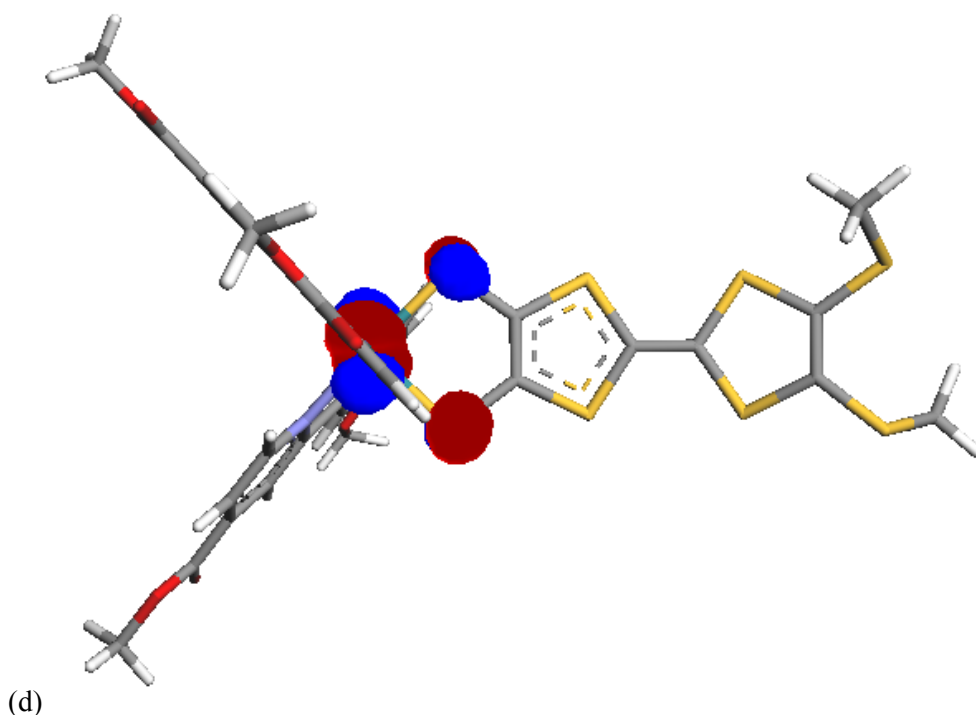A summary of those transitions with significant oscillator strength can be found in the supplementary information, Table S3. The lowest energy calculated transition was the HOMO-LUMO transition at 1100 nm. This was not observed in the experimental spectrum, presumably due to the poor orbital overlap between the HOMO, based on the TTF, and the LUMO, based on the bipyridyl ligand. The low probability of this transition was also indicated by the very low calculated oscillator strength of the transition.

The visible region absorption bands are relatively well reproduced, with the energies being quite similar to those observed experimentally. The intensities are however somewhat overestimated, as has been observed previously.[37] Interestingly these transitions were calculated to have pure MLCT character, involving transitions from the HOMO-3 to unoccupied orbitals. This would suggest that the dye behaves largely as the separate chromophore and electron-donor system, as outlined in Fig. 1**Error! Reference source not found.**, hich agrees with the emission study results. Therefore, in a DSSC if the injection of an electron into the conduction band of TiO_2 occurs after MLCT then the resultant hole will be on the ruthenium centre. However, as the TTF moiety is easier to oxidise than the ruthenium, then intramolecular charge transfer can readily

occur between the two units, shifting the location of the dye cation to the TTF ligand. The location of the hole further from the surface of the TiO$_2$ should then lead to a significantly longer-lived charge-separated state. The lower energy visible band has significant contribution from transitions which originate from the TTF based HOMO, and so the poor orbital overlap may be contributing to the low molar extinction coefficient in this region of the observed absorption spectrum.
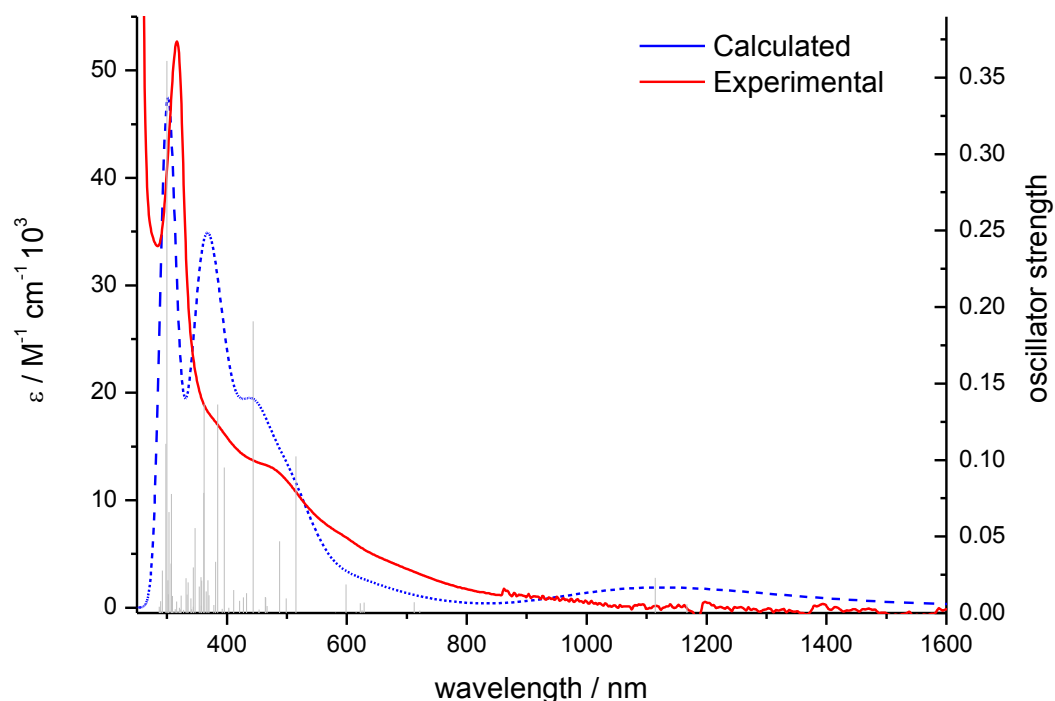
Figure 5. Gaussian convolution of calculated transitions (dotted blue line), compared to experimental spectrum (solid red line), for **2** in DMF, both left axis. The calculated transitions are also shown relative to the calculated oscillator strength (grey columns), right axis.

DSSC Measurements

Given the significant evidence for the high possibility of extended charge-separation , the I-V measurements for **3** were somewhat disappointing, with very low efficiencies recorded (Fig. S11, Table 4). Under the same conditions a DSSC sensitised with N719 achieved an efficiency of 2.65 %. The binding to the TiO$_2$ film by **3** was satisfactory with a dark brown film obtained after soaking the film overnight in a 0.5 mM 1:1 methanol/DMF solution. The absorption spectrum of the film resembled that of the dye in solution, indicating no degradation of the dye upon adsorption. Variation of the electrolyte from electrolyte A (see experimental)

to contain simply 0.6 M LiI/ 0.03 M I_2 showed no significant improvement, therefore an energy mismatch between the LUMO and the conduction band of the TiO_2 does not appear to be the cause of the low efficiency in this case. The failure of this dye to function efficiently in a DSSC is further discussed with respect to the transient absorption spectroscopy measurements.

Table 4. Short-circuit current, open-circuit voltage, fill factor and global efficiency for DSSCs sensitised with **3** and N719.

Cell	V_{oc} (mV)	I_{sc} (mA cm^{-2})	ff	η (%)
Electrolyte A	88	0.12	0.31	0.004
LiI/I_2 electrolyte	93	0.17	0.35	0.006
N719	737	6.87	0.53	2.65

Transient Absorption Spectroscopy

The clear growth of a band at ~ 1000 nm upon oxidation of **2**, observed in the OTTLE study, was used to investigate the charge-separated lifetime of the TiO_2 conduction band electron ($TiO_2|e^-$) and the dye cation hole (d^+) using transient absorption spectroscopy.

Using an excitation wavelength of 500 nm and a probe wavelength of 995 nm the charge-separated lifetime was studied using three different electrolytes: propylene carbonate (PC) only, propylene carbonate and lithium perchlorate and finally propylene carbonate and lithium iodide/iodine (Fig. 6). This allowed both the recombination and regeneration kinetics to be investigated.

An important issue to address was whether the addition of these additives to the electrolyte was causing degradation of the dye in some form. The absorption spectra of the sensitised TiO_2 films were recorded upon changing the electrolyte composition, before and after irradiation (Fig S12). There was found to be no change in absorbance of the film, and no absorbance at ~ 1000 nm which would interfere with the TAS study. This confirms that the species being observed involves the excited state of the dye or the dye cation specifically, and not the neutral form of the dye.

Initial results were very promising, with an extended lifetime observed during the recombination study using propylene carbonate only as the electrolyte. The measured half-life ($t_{1/2}$) was found to be very long with a value of 20 ms, compared to a $t_{1/2}$ = 600 μs for N719, under the same conditions. The addition of LiClO$_4$ to the electrolyte had two effects: the amplitude of the signal increased and the dynamics of the system became more complex. There is still a long-lived signal and also a secondary rise and decay of the signal at longer time scales. The study involving LiI/I_2 was found to have the same complex dynamics as the LiClO$_4$ recombination study, with only a small decrease in signal life-time, suggesting that the regeneration of this dye is particularly

slow. The failure of the iodide to rapidly regenerate the neutral dye is probably due to its insufficiently-positive oxidation potential and is likely to be the cause of the very low DSSC efficiency measured.
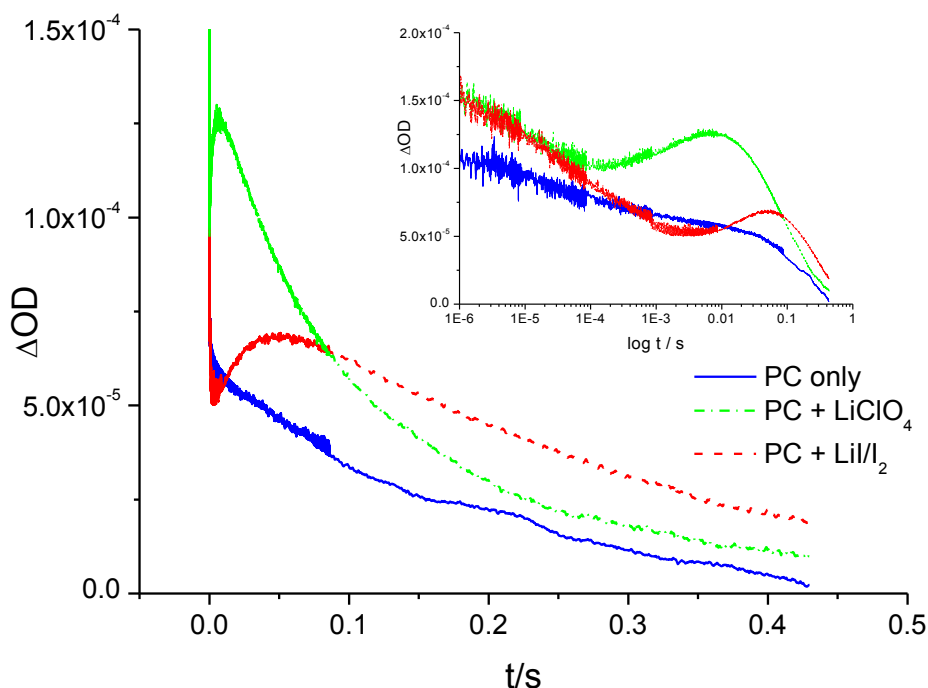

Figure 6. Transient absorption decay profiles for a TiO_2 film sensitised with **3**, using propylene carbonate (PC), PC + $LiClO_4$ and PC + LiI/I_2 as electrolytes. The excitation wavelength was 500 nm and probe wavelength 995 nm. The inset shows data plotted against log(t/s).

Li^+ has been shown to play an important role in the dynamics of dye reduction, with the electrostatic environment of the interface altering following charge injection.[38] In addition, recent evidence suggests that the formation of a ruthenium bipyridyl cation/iodide intermediate is an essential step for the re-reduction of the dye. [39,40] Thus the changes in the transient decay profile upon addition of both Li^+ and I^- may arise from varied interactions of the ions with the neutral and oxidised dye. The final decay in signal amplitude is ultimately due to the recombination of the injected electron with the oxidised dye, rather than regeneration of the neutral dye *via* reduction by the iodide.

To investigate this further, we used spectroelectrochemical studies to observe whether the dye was forming a distinctly different species in the presence of LiI. The mono-oxidised species was generated under standard OTTLE conditions in 0.1 M TBABF$_4$/DMF. Upon addition of 0.15 M LiI in DMF to the OTTLE cell however, regeneration of the neutral dye spectrum was observed. Under the long timescale of the scan used in

the OTTLE study (approximately 2 minutes), no intermediate species was observed. This study proves that LiI will regenerate **3** as desired, but it is also known from the TAS study that this does not occur faster than recombination *i.e.* below one second.

Conclusions

This work has shown the successful synthesis and characterisation of a series of ruthenium bipyridyl complexes with a covalently linked TTF moiety. The ester-functionalised analogue shows six chemically-stable redox states encompassing a charge of 3+ to 2- and all have been characterised spectroscopically. The absorption spectra of the complexes were found to be broad and with comparatively low molar extinction co-efficients in the visible region for all derivatives. Whilst this low absorption is not ideal for use in a DSSC, the nature of the orbitals in this series proved to have interesting effects on the behaviour in a DSSC. The HOMO was deduced to be largely TTF based *via* spectroelectrochemical and computational techniques. The computational work indicates the HOMO-1 also to be largely TTF based. The TD-DFT study showed the main origin of the low energy absorption band to be ruthenium to bipyridyl ligand MLCT, suggesting that these dyes are acting as a largely separate chromophore and electron donor unit as desired, which was also indicated by the emission studies.

Binding to TiO_2 by the acid derivative was successful and the behaviour of this dye in a DSSC proved to be very informative, despite the lack of efficient function. Investigation of the kinetics of recombination and regeneration *via* transient absorption spectroscopy, revealed the desired long-lived charge-separated state as well as inefficient regeneration, with the latter being the cause of the low efficiency. It was observed that the dye could be regenerated by iodide but only on a longer timescale than that of the recombination. Overall, dye **3** is rather unique in displaying a long lived charge-separated state under complete solar-cell conditions, with both charge recombination and charge regeneration occuring on a timescale of greater than 20 ms. We are not aware of any other dye with this property, and it may provide an ideal opportunity to study, in a complete solar cell, long-lived Dye$^+$/iodide interactions and/or slow re-organisation dynamics of the electrostatic environment of the dye-TiO_2 interface.

Experimental

(SC_2H_4CN)$_2$TTF(SMe)$_2$ and the ruthenium bis-bipyridyl dichloride starting complexes were prepared as described in the literature[41]. All solvents were reagent grade and were used as received.

OTTLE (Optically Transparent Thin Layer Electrode) measurements were taken using a quartz cell of 0.5 mm, a Pt/Rh gauze working electrode, an Ag/AgCl reference electrode and a Pt wire counter electrode. UV-

vis spectra were recorded on a Perkin-Elmer Lambda 9 spectrophotometer, controlled by a Datalink PC, running UV/Winlab software. 0.1 M TBABF$_4$ was used as the supporting electrolyte in all cases.

All *in-situ* EPR spectra were recorded on an X-band Bruker ER200D-SCR spectrometer, connected to datalink 486DX PC running EPR Acquisition System, version 2.42 software. *In-situ* EPR experiments were electrogenerated using a BAS CV-27 voltammograph. Variable temperature work was carried out using a Bruker ER111VT variable temperature unit. In some cases, solution spectra were recorded at reduced temperature to ensure long-term stability of the reduced species. All g values were corrected to 2,2'-diphenyl-1-picrylhydrazyl with $g_{literatue} = 2.0036 \pm 0.0002$.

The Gaussian 03 program was used to perform all calculations.[42] The Becke three parameters hybrid exchange and the Perdew-Wang 1991 correlation functionals (B3PW91) level of theory were used.[43,44] For the ruthenium atom a Hay-Wadt VDZ (n+1) ECP was used [45] and all other atoms were described by 6-31G*.[46] The initial structure was input using the builder program Arguslab.[47] A frequency calculation was performed to ensure the optimised structure was a minimum on the potential energy surface, verified by the absence of negative imaginary values. The molecular orbital isosurfaces were generated using the cubegen utility in Gaussian 03.

To make the DSSCs titanium dioxide paste (Dyesol, DSL-18NR-T) was deposited onto cleaned fluorine doped tin oxide conductive glass (TEC 8, Pilkington, UK) by doctor-blading. The film was dried at 100 ^{o}C for 15 minutes and then sintered at 450 ^{o}C for 30 minutes to remove the organics and to form a mesoporous film structure. The thickness of the film was about 12 μm. The films were sensitized with **3** using a 0.5 mM solution of the dye in methanol. The platinized counter electrode was fabricated following the previously reported procedure.[48] The cell was completed by sealing the dye coated TiO$_2$ electrode and Pt electrode of a cell together by a thermal plastics spacer (Surlyn 1702, 25 μm, Solaronix) at 120°C. The electrolyte was introduced into the cell through the two holes which were drilled in the counter electrode. The holes were subsequently sealed by the thermal plastics (Surlyn 1702, Solaronix) combined with a piece of microscope slide under press. The active area of the cell was 1 cm^2. The default electrolyte composition (electrolyte A) was 0.6 M 1-methyl-3-propylimidazolium iodide (PMII), 0.03 M I$_2$, 0.1 M guanidinium thiocyanate, 0.5 M tert-butyl pyridine (TBP) in acetonitrile/valeronitrile.

Transient absorption decays were measured using the "flash photolysis" technique. The sample was excited with a dye laser (Photon Technology International Inc., GL-301) pumped by a nitrogen laser (Photon Technology International Inc., GL-3300). The excitation wavelength was 500 nm. The pulse width was 800 ps, the fluence was about 50 μJcm^{-2} and the repetition frequency was 1 Hz. A 100-W tungsten-halogen lamp (Bentham, IL1) with a stabilized power supply (Bentham, 605) was used as a probe light source. The probe light passing through the sample was detected with a silicon photodiode (Hamamatsu Photonics, S1722-01). The signal from the photodiode was pre-amplified and sent to the main amplification system with an

electronic band-pass filter to improve signal to noise ratio (Costronics Electronics). The amplified signal was collected with a digital oscilloscope (Tektronix, TDS 220), which was synchronized with a trigger signal of the laser pulse from a photodiode (Thorlabs Inc., DET210). To reduce stray light, scattered light and emission from the sample, two monochromators and appropriate optical cut-off filters were placed before and after the sample. Owing to the amplification and noise reduction system, the detectable change of absorbance was as small as 10^{-5} to 10^{-6}.

2,3-bis(2-cyanoethylthio)-6,7-bis(methylthio)tetrathiafulvelene (TTF(SMe₂)). CHN Calc. for $C_{14}H_{14}N_2S_8$: C 36.02, H 3.02, N 6.0, Found: C 36.69, H 3.34, N 5.11. ^{1}H-NMR (DMSO, 250 MHz): δ 3.04 (t, J_{HH} = 7, 4H), 2.72 (t, J_{HH} = 6, 4H), 2.37 (s, 6H).

Ru(bpy)₂(TTF(SMe)₂) (1). Ru(bpy)₂Cl₂ (100 mg, 0.2 mmol) was dissolved in methanol (10 ml) and silver nitrate (71 mg, 0.4 mmol) in water (1 ml) was added. The mixture was refluxed for 1 hour and the resulting white silver chloride precipitate removed by centrifuge. TTF(SMe₂) (93 mg, 0.2 mmol) was suspended in tetrahydrofuran (5 ml), at 0 °C under nitrogen, and a 25 % tetramethylammonium hydroxide solution in methanol (250 μl, xs) added. The mixture was stirred under nitrogen at 0 °C for 20 minutes, followed by the removal of the solvent *in vacuo* and the resulting solid was redissolved in methanol (5 ml). The red ruthenium bipyridyl filtrate was then quickly added to the TTF(SMe₂) solution and the mixture stirred for 3 hours. The resulting brown product was collected by filtration. Yield: 61 mg (40 %). The crude product was further purified *via* a Sephadex LH-20 column using a 50:50 solution of methanol/dimethylformamide as the eluent. CHN Calc. for $C_{28}H_{28}N_4S_8Ru$: C 40.71, H 3.42, N 6.78, Found: C 40.86, H 2.99, N 6.57. +ve FAB-MS: m/z 772 (M$^+$). ^{1}H-NMR (DMSO, 360 MHz): δ 10.68 (d, J_{HH} = 5, 2H), 9.75 (d, J_{HH} = 8, 2H), 8.61 (t, J_{HH} = 8, 2H), 8.10 (d, J_{HH} = 8, 2H), 7.97 (t, J_{HH} = 6, 2H), 7.80 (t, J_{HH} = 6, 2H), 7.46 (d, J_{HH} = 6, 2H), 7.34 (t, J_{HH} = 7, 2H), 2.42 (s, 6H).

Ru(decbpy)₂(TTF(SMe)₂) (2). Ru(decbpy)₂Cl₂ (100 mg, 0.129 mmol) was dissolved in methanol (10 ml) and silver nitrate (44 mg, 0.26 mmol) in water (1 ml) was added. The mixture was refluxed for 1 hour and the resulting white silver chloride precipitate removed by centrifuge. TTF(SMe₂) (60 mg, 0.129 mmol) was suspended in tetrahydrofuran (5 ml), at 0 °C under nitrogen, and a 25 % tetramethylammonium hydroxide solution in methanol (120 μl, xs) added. The mixture was stirred under nitrogen at 0 °C for 20 minutes, followed by the removal of the solvent *in vacuo* and the resulting solid was redissolved in methanol (5 ml). The red ruthenium bipyridyl filtrate was then quickly added to the TTF(SMe₂) solution and the mixture stirred for 2 hours. The resulting brown product was collected by filtration. Yield: 67 mg (49 %). The crude product

was further purified *via* a Sephadex LH-20 column using a 50:50 solution of methanol/dimethylformamide as the eluent. CHN Calc. for $C_{44}H_{46}N_4S_8O_8RuCl_8$: C 37.63, H 3.59, N 3.99, Found: C 37.78, H 2.56, N 4.23. +ve FAB-MS: m/z 1060 (M^+). ^{1}H-NMR (DMSO, 360 MHz): δ 10.12 (d, J_{HH} = 6, 2H), 9.14 (s, 2H), 8.95 (s, 2H), 8.27 (d, J_{HH} = 6, 2H), 7.78 (d, J_{HH} = 6, 2H), 7.5 (d, J_{HH} = 6, 2H), 4.54 (q, J_{HH} = 7, 2H), 4.37 (q, J_{HH} = 7, 2H), 2.41 (s, 6H), 1.46 (t, J_{HH} = 7, 3H), 1.32 (t, J_{HH} = 7, 3H).

Ru(dcbpy)₂(TTF(SMe)₂) (3). Ru(decbpy)$_2$Cl$_2$ (100 mg, 0.129 mmol) dissolved in methanol (10 ml) and silver nitrate (44 mg, 0.26 mmol) in water (1 ml) added. The mixture was refluxed for 1 hour and the resulting white silver chloride precipitate removed by centrifuge. The filtrate was treated with 0.1 M KOH (3 ml) and the mixture stirred for 15 mins. TTF(SMe$_2$) (60 mg, 0.129 mmol) was suspended in tetrahydrofuran (5 ml), at 0 °C under nitrogen, and a 25 % tetramethylammonium hydroxide solution in methanol (120 μl, xs) added. The mixture was stirred under nitrogen at 0 °C for 20 minutes, followed by the removal of the solvent *in vacuo* and the resulting solid was redissolved in methanol (5 ml). The base treated ruthenium bipyridyl filtrate was then quickly added to the TTF(SMe$_2$) solution and the mixture stirred for 2 hours. On acidification of the mixture with 1 M HCl (2 ml) a brown precipitate was collected by centrifugation. Yield: 64 mg (56 %). The crude product was further purified *via* a Sephadex LH-20 column using a 50:50 solution of methanol/dimethylformamide as the eluent. CHN Calc. for $C_{32}H_{26}N_4S_8O_{10}Ru$: C 39.05, H 2.66, N 5.69, Found: C 38.82, H 2.00, N 4.65. ^{1}H-NMR (DMSO, 360 MHz): δ 10.06 (d, J_{HH} = 6, 2H), 9.05 (s, 2H), 8.96 (s, 2H), 8.20 (d, J_{HH} = 6, 2H), 7.72 (d, J_{HH} = 6, 2H), 7.46 (d, J_{HH} = 6, 2H), 2.36 (s, 6H).

References

[1] Md.K. Nazeeruddin, M. Grätzel, *Comp. Coord. Chem. II* 2003, **9**, 719; N. Roberston, *Angew. Chem. Int. Ed*. 2006, **45**, 2338-2345

[2] R. Argazzi, C.A. Bignozzi, T.A. Heimer, F.N. Castellano, G.J. Meyer, *J. Phys. Chem. B*, 1997, **101**, 2591-2597.

[3] R. Argazzi, C.A. Bignozzi, T.A. Heimer, F.N. Castellano, G.J. Meyer, *J. Am. Chem. Soc.*, 1995, **117**, 11815-11816.

[4] N. Hirata, J-J. Lagref, E.J. Palomares, J.R. Durrant, Md. K. Nazeeruddin, M. Grätzel, D. Di Censo, *Chem. Eur. J.*, 2004, **10**, 595-602.

[5] K. Peter, H. Wietasch, B. Peng, M. Thelakkat, *Appl. Phys. A*, 2004, **79**, 65-71.

[6] S.A. Haque, S. Handa, K. Peter, E. Palomares, M. Thelakkat, J.R. Durrant, *Angew. Chemie Int. Ed.,* 2005, **44**, 5740-5744.

[7] C.S. Karthikeyan, K. Peter, H. Wietasch, M. Thelakkat, *Sol. Energy Mater. Sol. Cells*, 2007, **91**, 432-439.

[8] S. Handa, H. Wietasch, M. Thelakkat, J.R. Durrant, S.A. Haque, *Chem. Commun*., 2007, 1725-1727.

[9] K. Shankar, J. Bandara, M. Paulose, H. Wietasch, O.K. Varghese, G.K. Mor, T.J. LaTempa, M. Thelakkat, C.A. Grimes, *Nano Lett.*, 2008, **8**, 1654-1659.

[10] C.S. Karthikeyan, H. Wietasch, M. Thelakkat, *Adv. Mater.*, 2007, **19**, 1091-1095.

[11] J.N. Clifford, E. Palomares, Md.K. Nazeeruddin, M. Grätzel, J. Nelson, X. Li, N.J. Long, J.R. Durrant, *J. Am. Chem. Soc.*, 2004, **126**, 5225-5233.

[12] M.R. Bryce, *Chem. Soc. Rev.*, 1994, **20**, 355-390.

[13] M. Bendikov, F. Wudl, D.F. Perepichka, *Chem. Rev.*, 2004, **104**, 4891-4945.

[14] M. Mas-Torrent, C. Rovira, *J. Mater. Chem.,* 2006, **16**, 433-436.

[15] T. Enoki, A. Miyazaki, *Chem. Rev.*, 2004, **104**, 5449-5477.

[16] T. Jørgenson, T.K. Hansen, J. Becher, *Chem. Soc. Rev.*, 1994, **23**, 41-51.

[17] J. Becher, Z-T. Li, P. Blanchard, N. Svenstrup, J. Lau, M.B. Nielsen, P. Leriche, *Pure & Appl. Chem.*, 1997, **69**, 465-470.

[18] T. Devic, D. Rondeau, Y. Şahin, E. Levillain, R. Clérac, P. Batail, N. Avarvari, *Dalton Trans.*, 2006, 1331-1337.

[19] Q-Y. Zhu, Y. Liu, Y. Zhang, G-Q. Bian, G-Y. Niu, J. Dai, *Inorg. Chem.*, 2007, **46**, 10065-10070.

[20] N. Martinez Rivera, E.M. Engler, R.R. Schumaker, *Chem. Commun.*, 1979, 184-185.

[21] L.V. Interrante, K.W. Browall, H.R. Hart, I.S. Jacobs, G.D. Watkins, S.H. Wee, *J. Am. Chem. Soc.*, 1975, **97**, 889-890.

[22] T. Nakazono, M. Nakano, H. Tamura, G. Matsubayashi, *J. Mater. Chem.*, 1999, **9**, 2413-2417.

[23] Y. Suga, M. Nakano, H. Tamura, G. Matsubayashi, *Bull. Chem. Soc. Jpn.*, 2004, **77**, 1877-1883.

[24] Y. Ji, R. Zhang, Y-J. Li, J-L. Zuo, X-Z. You, *Inorg. Chem.*, 2007, **46**, 866-873.

[25] S. Campagna, S. Serroni, F. Puntoriero, F. Loiseau, L. De Cola, C.J. Kleverlaan, J. Becher, A.P. Sørenson, P. Hascoat, N. Thorup, *Chem. Eur. J.*, 2002, **8**, 4461-4469.

[26] C. Goze, S-X. Liu, C. Leiggener, L. Sanguinet, E. Levillain, A. Hauser, S. Decurtins, *Tetrahedron*, 2008, **64**, 1345-1350.

[27] C. Jia, S-X. Liu, C. Tanner, C. Leiggener, A. Neels, L. Sanguinet, E. Levillain, S. Leutwyler, A. Hauser, S. Decurtins, *Chem. Eur. J.*, 2007, **13**, 3804-3812.

[28] C. Goze, C. Leiggener, S-X. Liu, L. Sanguinet, E. Levillain, A. Hauser, S. Decurtins, *Chem. Phys. Chem.*, 2007, **8**, 1504-1512.

[29] R.R. Ruminski, B.F. Ermel, M.A. Hiskey, *Inorg. Chim. Acta*, 1986, **119**, 195-201.

[30] K. Natsuaki, M. Nakano, G. Matsubayashi, R. Arakawa, *Inorg. Chim. Acta,* 2000, **299**, 112-117.

[31] P.R. Ashton, V. Balzani, J. Becher, A. Credi, M.C.T. Fyfe, G. Mattersteig, S. Menzer, M.B. Nielsen, F.M. Raymo, J.F. Stoddart, M. Venturi, D.J. Williams, *J. Am. Chem. Soc.*, 1999, **121**, 3951-3957.

[32] K. Kalyanasundaram, *Coord. Chem. Rev.*, 1982, **46**, 159-244.

[33] J. Ferguson, E. Krausz, *J. Phys. Chem.*, 1987, **91**, 3161-3167.

[34] Md.K. Nazeeruddin, K. Kalyanasundaram, *Inorg. Chem.*, 1989, **28**, 4251-4259.

[35] N.H. Damrauer, G. Cerullo, A. Yeh, T.R. Boussie, C.V. Skank, J.K. McCusker, *Science*, 1997, **275**, 54-57.

[36] G. Wolfbauer, A.M. Bond, D.R. MacFarlane, *Inorg. Chem.*, 1999, **38**, 3836-3846.

[37] K.L. McCall, J.R. Jennings, H. Wang, A. Morandeira, L.M. Peter, J.R. Durrant, L.J. Yellowlees, J.D. Woollins, N. Robertson, *J.Photochem. Photobiol A: Chem.*, 2009, **202**, 196.

[38] A. Staniszewski, S. Ardo, Y. Sun, F. N. Castellano, G. J. Meyer, *J. Am. Chem. Soc.,* 2008, **130**, 11586

[39] I. Montanari, J. Nelson, J.R. Durrant, *J. Phys. Chem. B*, 2002, **106**, 12203-12210.

[40] J.N. Clifford, E. Palomares, Md.K. Nazeeruddin, M. Grätzel, J.R. Durrant, *J. Phys. Chem. C*, 2007, **111**, 6561-6567.

[41] K.B. Simonsen, N. Svenstrup, J. Lau, O. Simonsen, P. Mork, G.J. Kristensen, J. Becher, *Synth.*, 1996, 407-418.

[42] Gaussian 03, Revision C.02, M. J. Frisch, G. W. Trucks, H. B. Schlegel, G. E. Scuseria, M. A. Robb, J. R. Cheeseman, J. A. Montgomery, Jr., T. Vreven, K. N. Kudin, J. C. Burant, J. M. Millam, S. S. Iyengar, J. Tomasi, V. Barone, B. Mennucci, M. Cossi, G. Scalmani, N. Rega, G. A. Petersson, H. Nakatsuji, M. Hada, M. Ehara, K. Toyota, R. Fukuda, J. Hasegawa, M. Ishida, T. Nakajima, Y. Honda, O. Kitao, H. Nakai, M. Klene, X. Li, J. E. Knox, H. P. Hratchian, J. B. Cross, V. Bakken, C. Adamo, J. Jaramillo, R. Gomperts, R. E. Stratmann, O. Yazyev, A. J. Austin, R. Cammi, C. Pomelli, J. W. Ochterski, P. Y. Ayala, K. Morokuma, G. A. Voth, P. Salvador, J. J. Dannenberg, V. G. Zakrzewski, S. Dapprich, A. D. Daniels, M. C. Strain, O. Farkas, D. K. Malick, A. D. Rabuck, K. Raghavachari, J. B. Foresman, J. V. Ortiz, Q. Cui, A. G. Baboul, S. Clifford, J. Cioslowski, B. B. Stefanov, G. Liu, A. Liashenko, P. Piskorz, I. Komaromi, R. L. Martin, D. J. Fox, T. Keith, M. A. Al-Laham, C. Y. Peng, A. Nanayakkara, M. Challacombe, P. M. W. Gill, B. Johnson, W. Chen, M. W. Wong, C. Gonzalez, and J. A. Pople, Gaussian, Inc., Wallingford CT, 2004.

[43] J.P. Perdew, J.A. Chevary, S.H. Vosko, K.A. Jackson, M.R. Pederson, D.J. Singh, C. Fiolhais, *Phys. Rev. B*, 1993, **48**, 4978-4978.

[44] J.P. Perdew, K. Burke, Y. Wang, *Phys. Rev. B*, 1996, **54**, 16533-16539.

[45] P.J. Hay, W.R. Wadt, *J. Chem. Phys.*, 1985, **82**, 299-310.

[46] M.M. Francl, W.J. Pietro, W.J. Hehre, J.S. Binkley, M.S. Gordon, D.J. Defrees, J.A. Pople, *J. Chem. Phys.,* 1982, **77**, 3654-3665.

[47] Arguslab 4.0, M.A. Thompson, Planaria Software LLC, Seattle, http://www.arguslab.com.

[48] N. Papageorgiou, W.F. Maier, M. Grätzel, J. Electrochem. Soc. 1997, **144** 876-884.